

# RSC Advances



This is an *Accepted Manuscript*, which has been through the Royal Society of Chemistry peer review process and has been accepted for publication.

*Accepted Manuscripts* are published online shortly after acceptance, before technical editing, formatting and proof reading. Using this free service, authors can make their results available to the community, in citable form, before we publish the edited article. This *Accepted Manuscript* will be replaced by the edited, formatted and paginated article as soon as this is available.

You can find more information about *Accepted Manuscripts* in the [Information for Authors](#).

Please note that technical editing may introduce minor changes to the text and/or graphics, which may alter content. The journal's standard [Terms & Conditions](#) and the [Ethical guidelines](#) still apply. In no event shall the Royal Society of Chemistry be held responsible for any errors or omissions in this *Accepted Manuscript* or any consequences arising from the use of any information it contains.



## Direct methylation of N-Methylaniline with CO<sub>2</sub>/H<sub>2</sub> catalyzed by gold nanoparticles supported on alumina

Gao Tang,<sup>a</sup> Hong-Liang Bao,<sup>b</sup> Chan Jin,<sup>b</sup> Xin-Hua Zhong\*<sup>a</sup> and Xian-Long Du\*<sup>b</sup>

Received 00th January 20xx,  
Accepted 00th January 20xx

DOI: 10.1039/x0xx00000x

www.rsc.org/

Small gold nanoparticles (~ 3 nm) loaded onto various supports have been prepared by a deposition-precipitation method and studied for direct methylation of N-methylaniline with CO<sub>2</sub>/H<sub>2</sub>. Among the catalysts examined, an acid-base bifunctional support  $\gamma$ -alumina supported gold catalyst (Au/ $\gamma$ -Al<sub>2</sub>O<sub>3</sub>) exhibits the best catalytic performance. Au/ $\gamma$ -Al<sub>2</sub>O<sub>3</sub> catalysts with controlled mean Au particle sizes (1.8–8.3 nm) have also been successfully prepared by regulating concentration of HAuCl<sub>4</sub> in solution, aging time, aging temperature and mole ratio of urea to gold in the process of deposition-precipitation with urea. The turnover frequency (TOF) values for direct methylation of N-methylaniline with CO<sub>2</sub>/H<sub>2</sub> increase with decreasing the mean size of Au nanoparticles (from 8.3 to 1.8 nm), showing that methylation of N-methylaniline with CO<sub>2</sub>/H<sub>2</sub> is a structure-sensitive reaction. A fast increase in TOF occurs when the mean Au particle size becomes smaller than 3 nm. Through TEM (transmission electron microscope), gold L<sub>3</sub>-edge XAFS (X-ray absorption fine structure) and CO<sub>2</sub>- and NH<sub>3</sub>-TPD (temperature programmed desorption) analysis, we can conclude the Au particle sizes, oxidation state of gold species and acid-base properties of supports are responsible for the high catalytic activity of direct methylation of N-methylaniline with CO<sub>2</sub>/H<sub>2</sub>.

### Introduction

Carbon dioxide (CO<sub>2</sub>) is one of the greenhouse gases and the accumulation of a huge amount of CO<sub>2</sub> has caused significant and negative effects on the global environment.<sup>1</sup> It is crucial, therefore, to take effective measures to reduce CO<sub>2</sub> emission and utilize CO<sub>2</sub> resource. In this regard, carbon dioxide has been used as an inexpensive and nontoxic C<sub>1</sub> feedstock for producing commodity chemicals, fuels and various materials in the last decades.<sup>2–4</sup> Owing to its thermodynamic stability, highly efficient activation of CO<sub>2</sub> and a strong thermodynamic driving force are required for efficient transformation of CO<sub>2</sub>. In this respect, only a handful of industrial processes have been realized for CO<sub>2</sub> utilization, such as the production of urea, salicylic acid, and carbonates.<sup>5</sup> Additionally, the catalytic hydrogenation of CO<sub>2</sub> to methanol, formic acid or its derivatives have been reported by using various catalysts.<sup>6,7</sup> Carbon dioxide can also be converted into cyclic carbonates,<sup>8</sup> dimethyl carbonate (DMC),<sup>9</sup> formamides<sup>10</sup> and carboxylic acids,<sup>11</sup> activated by relevant reactive substrates such as

epoxides, alcohols, amines and olefins respectively.

Methylamines, including dimethylamine, trimethylamine, methylamine and dimethylformamide (DMF), have been usually used as platform chemicals for preparing fertilizers, fungicides, synthetic leathers or polymers.<sup>12</sup> Hazardous alkylating agents, such as methyl iodide, dimethyl sulfate, and dimethyl carbonate, are traditionally preferred for the preparation of methylamines.<sup>13</sup> Meanwhile, dimethylsulfoxide and formic acid have also been found to be the available carbon sources for methylation of amines by catalysts.<sup>14</sup> Great efforts on the other hand have been made to develop new catalytic process for preparation of N-methylated compounds using CO<sub>2</sub> as a C<sub>1</sub> building block in the absence of the toxic alkylating agents. In early 2013, two catalytic systems were independently reported by two research groups for the methylation of amines with CO<sub>2</sub> and silanes by homogeneous catalysts, producing siloxane as a by-product.<sup>15</sup> Shortly afterwards, a green method for methylation of amines with CO<sub>2</sub>/H<sub>2</sub> has been reported using homogeneous Ru-based catalysts by the groups of Klankermayer and Beller, generating water as the only by-product.<sup>16</sup> Lately, two new metal-free homogeneous catalysts for methylation of amines using CO<sub>2</sub> as a C<sub>1</sub> source, were developed by the groups of Dyson and Cantat.<sup>17</sup> Despite the significant progress that has been made in the area of amine methylation using CO<sub>2</sub>/H<sub>2</sub> with homogeneous systems, there are still few available relevant reports on the heterogeneously catalyzed methylation of amines with CO<sub>2</sub>/H<sub>2</sub>. Recently, N-methylation of amines with CO<sub>2</sub>/H<sub>2</sub> was realized by heterogeneous catalysts such as CuAlO<sub>x</sub>,<sup>18</sup> Pt-MoO<sub>x</sub>/TiO<sub>2</sub><sup>19</sup> and Pd/CuZrO<sub>x</sub><sup>20</sup> respectively. These

<sup>a</sup> Key Laboratory for Advanced Materials, Institute of Applied Chemistry  
East China University of Science and Technology  
Shanghai 200237 (P.R. China)  
zhongxh@ecust.edu.cn

<sup>b</sup> Key Laboratory of Interfacial Physics and Technology  
Shanghai Institute of Applied Physics  
Chinese Academy of Sciences  
Jialuo Road 2019, Shanghai 201800 (P.R. China)  
E-mail: duxianlong@sinap.ac.cn

Electronic Supplementary Information (ESI) available: Details containing figures of TEM, catalysis activity, XRD. See DOI: 10.1039/x0xx00000x

heterogeneous systems however are limited by their low turnover frequencies (TOF,  $< 3.3\text{h}^{-1}$ ) and prolonged reaction times (24–48 h) for achieving the high product yields ( $> 75\%$ ).

Catalysts based on supported gold nanoparticles (NPs) have been found to be versatile catalysts for many chemical transformations in various mild chemical processes, since Haruta and his associates discovered gold particles ( $< 5\text{nm}$ ) supported on transition metal oxides were very active for CO oxidation at low temperature.<sup>21</sup> It is generally accepted that the mean size of gold NPs, supports and preparation methods markedly influence the catalytic performances of supported gold catalysts.<sup>22</sup> Bus et al. reported that small gold particles (size  $< 2\text{nm}$ ) loaded on  $\gamma\text{-Al}_2\text{O}_3$  were active for selective hydrogenation of cinnamaldehyde to cinnamyl alcohol.<sup>23</sup> It was previously reported that both size and support of supported gold catalyst affected the reaction rates for the water-gas shift reaction.<sup>24</sup> Sun et al showed that basic resin R201 supported Au catalyst displayed good performance in the one-pot synthesis of styrene carbonate from styrene and  $\text{CO}_2$ .<sup>25</sup> Recently, Liu et al has reported the effective synthesis of benzimidazoles from 2-nitroanilines and  $\text{CO}_2/\text{H}_2$  using supported gold catalyst.<sup>26</sup> Besides, as reported by the group of Manzoli, gold sites were essential for hydrogen dissociation on metal oxide supports, which could activate hydrogen.<sup>27</sup> These established knowledge provide inspiration for our current study of methylation of N-methylaniline using  $\text{CO}_2/\text{H}_2$  with supported gold catalysts.

We previously reported that  $\text{Au}/\text{Al}_2\text{O}_3\text{-VS}$  (very small gold NPs loaded on  $\gamma\text{-Al}_2\text{O}_3$ ) catalyzed direct methylation of aniline using  $\text{CO}_2/\text{H}_2$  with total conversion of aniline and excellent selectivity towards N, N-dimethylaniline (92%) at  $140^\circ\text{C}$  for 7 h.<sup>28</sup> To the best of our knowledge, it is the highest TOF value ever reported to date for methylation of aniline with  $\text{CO}_2/\text{H}_2$  in this catalysis system based total gold atoms ( $26\text{h}^{-1}$ ). Small Au NPs ( $\sim 2\text{nm}$ ) supported on alumina is critical for high activity for methylation of amines using  $\text{CO}_2/\text{H}_2$ , in comparison with Au NPs supported on other supports.<sup>28</sup> We herein extend the previous work, and systematically study the effects of the mean size of Au NPs, gold species and acid-base properties of supports on catalytic activity of  $\text{Au}/\text{Al}_2\text{O}_3$  catalyst for direct methylation of N-methylaniline with  $\text{CO}_2/\text{H}_2$ . We have also examined the mechanism of methylation of N-methylaniline in the presence of  $\text{CO}_2/\text{H}_2$  catalyzed by  $\text{Au}/\text{Al}_2\text{O}_3$  catalyst.

## Experimental

### Chemicals

Commercially available organic and inorganic compounds were used without further purification. Gold catalysts including 1 wt%  $\text{Au}/\text{TiO}_2$  (Catalogue number 79-0165), 1 wt%  $\text{Au}/\text{ZnO}$  (catalogue number 79-0170) were supplied by Mintek.

### Synthesis of $\text{Al}_2\text{O}_3$ , $\text{Mn}_2\text{O}_3$ and $\text{Co}_3\text{O}_4$ supports

$\text{Al}_2\text{O}_3$  powders were prepared by a conventional precipitation method. 45.0 g  $\text{Al}(\text{NO}_3)_3\cdot 9\text{H}_2\text{O}$  was dissolved in 500 mL deionized water at room temperature, the pH was adjusted to 9.0 by dropwise addition of  $\text{NH}_4\text{OH}$  (2.5 M). The resultant hydro gel was

washed with deionized water until free of  $\text{NO}_3^-$  ions. The precipitate was then dried at  $110^\circ\text{C}$  overnight and calcined at  $500^\circ\text{C}$  for 4 h in air. Then the particles were passed a 200-mesh sieve to get the qualities of particles with diameters of less than 0.074 millimeter. The crystal structure of  $\text{Al}_2\text{O}_3$  was gamma phase (based on XRD analysis, see Fig. S1).

$\text{Mn}_2\text{O}_3$  powders were prepared by calcination of  $\text{MnCO}_3$  sample (AR) at  $500^\circ\text{C}$  in flowing air (1 atm) for 4 h and then cooled.<sup>29</sup>

$\text{Co}_3\text{O}_4$  powders were prepared by a conventional precipitation method. 10.0 g  $\text{Co}(\text{NO}_3)_2\cdot 6\text{H}_2\text{O}$  was dissolved in 200 mL deionized water at room temperature, the pH was adjusted to 9.0 by dropwise addition of  $\text{NH}_4\text{OH}$  (2.5 M). The resultant hydro gel was washed with deionized water and dried at  $110^\circ\text{C}$  overnight. The product was calcined at  $400^\circ\text{C}$  for 4 h in air and then cooled.

### Catalyst synthesis

The theoretical Au loading for each catalyst used in this work was 1 wt%, unless otherwise stated.  $\text{Au}/\text{SiO}_2$  was prepared according to sonication-aided impregnation method reported by Wang et al.<sup>30</sup> The calculated amount of  $\text{SiO}_2$  (Degussa, Aerosil 380, specific surface area:  $380\text{m}^2\text{g}^{-1}$ ) was suspended in an aqueous solution of  $\text{HAuCl}_4$ , and the suspension was placed into the sonication bath with irradiation at 40 kHz and 200 W output power. After sonication, the water was removed by evaporation at  $80^\circ\text{C}$ . The solid powder was finally reduced in  $\text{H}_2$  atmosphere at  $350^\circ\text{C}$  for 2 h. The deposition-precipitation with urea method was used for the preparation of  $\text{Au}/\text{Al}_2\text{O}_3$ ,  $\text{Au}/\text{MgO}$ ,  $\text{Au}/\text{Co}_3\text{O}_4$ ,  $\text{Au}/\text{Mn}_2\text{O}_3$  and  $\text{Au}/\text{CeO}_2$  catalysts. In a typical procedure, urea was dissolved in  $\text{HAuCl}_4$  solution at room temperature. The support was then added to this clear solution, and the temperature of the resulting slurry was increased gradually to a fixed temperature. The temperature was maintained for a certain time. After cooling to room temperature, the solid was recovered by filtering and washing several times with distilled water. The sample was dried under vacuum at  $50^\circ\text{C}$  for 12 h, followed by reduction with a stream of 5 vol%  $\text{H}_2/\text{Ar}$  at  $350^\circ\text{C}$  for 2 h. The standard conditions were as follows:  $[\text{HAuCl}_4] = 0.48\text{mmol L}^{-1}$ ; aging time = 6 h; aging temperature =  $80^\circ\text{C}$ ; mole ratio of urea to Au = 200. The concentration of gold by weight was confirmed by ICP-AES.

### Characterization

Au loadings in all of the catalysts were measured by ICP-AES with an ICAP 6300 instrument when the sample was dissolved in aqua regia and diluted with distilled water to the proper concentration. The crystal structures of the prepared catalysts were characterized with powder X-ray diffraction (XRD) on a Bruker D8 Advance X-ray diffractometer using the Ni-filtered  $\text{Cu K}\alpha$  radiation source at 40 kV and 40 mA. TEM images for supported gold catalysts were taken with a Tecnai G2 electron microscope operating at 200 kV. Before being transferred into the TEM chamber, the samples dispersed with ethanol were deposited onto a carbon-coated copper grid and then quickly moved into the vacuum evaporator. The size distribution of the metal nanoclusters was determined by measuring about 200 random particles on the images.  $\text{NH}_3\text{-TPD}$  and  $\text{CO}_2\text{-TPD}$  were performed on an AutoChem 2950 HP instrument. Typically, the sample loaded in a quartz reactor was pretreated with high purity He at  $300^\circ\text{C}$  for 1 h. After cooling the sample to  $50^\circ\text{C}$ ,  $\text{NH}_3$  adsorption was performed by switching the He flow to a  $\text{NH}_3\text{-}$

He (10 vol% NH<sub>3</sub>) gas mixture and then maintaining the sample at 50 °C for 1 h. The gas-phase (and/or weakly adsorbed) NH<sub>3</sub>, was purged by high-purity He at the same temperature. NH<sub>3</sub>-TPD was then performed in the He flow by raising the temperature to 700 °C at a rate of 10 °C min<sup>-1</sup>. The desorbed NH<sub>3</sub> molecules were detected by using a MKS Cirrus 2 mass spectrometer at the signal of m/z 17. CO<sub>2</sub>-TPD was performed by using a similar procedure. The X-ray absorption data at the Au L-edge of the samples were recorded at room temperature in transmission mode using ion chambers at beam line BL14W1 of the Shanghai Synchrotron Radiation Facility (SSRF), China. The synchrotron radiation was monochromatized with a Si (111) double crystal monochromator, and mirrors were used to eliminate higher harmonics. The incident and transmitted beam intensities were monitored using ionization chambers filled with pure N<sub>2</sub>. During the measurement, the synchrotron was operated at energy of 3.5 GeV and a current of 250 mA. Data processing was performed using the program ATHENA and ARTEMIS. The X-ray absorption near-edge structure (XANES) was normalized with edge height and the first-order derivatives was taken to compare variation of absorption edge energies.

### Catalytic testing

A mixture of solvent (10 mL), N-methylaniline (1.0 mmol), and supported Au catalysts (Au 2.7-5.0 μmol) were charged into a 50-mL Hastelloy-C high pressure Parr reactor. The reactor was then exchanged with H<sub>2</sub>, followed by introducing 1.0 MPa CO<sub>2</sub> and 3.0 MPa H<sub>2</sub>. The reaction was reacted at desired temperature for given reaction time under magnetic stirring. Subsequently, the autoclave was cooled to room temperature, and n-octane (1 mmol, internal standard) was added for quantitative analysis by GC-FID (Agilent 7820A).

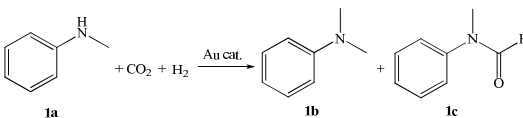
## Results and Discussion

### Solvent and support effects

In the course of identifying and optimizing key reaction parameters for N-methylaniline (**1a**) with CO<sub>2</sub>/H<sub>2</sub>, several solvents were investigated. The Au/γ-Al<sub>2</sub>O<sub>3</sub> catalyst with very small Au NPs (2.0 nm) was used as the standard catalyst. The highest yield of N, N-dimethylaniline (**1b**) was obtained when cyclohexane was used as the reaction medium (Table 1, entry 1). In contrast, the reaction in hexane, toluene, 1,4-Dioxane, CH<sub>2</sub>Cl<sub>2</sub> and THF (Table 1, entries 2-6) gave moderate to good yield (24-61 %) with excellent selectivity towards **1b** (> 90%), and in ethanol (Table 1, entry 7) obtained the lowest yield (2%) with poor selectivity towards **1b** (18%). Based on above results, we empirically concluded that the use of apolar solvents for direct methylation of **1a** with CO<sub>2</sub>/H<sub>2</sub> gave better conversion than the use of polar solvents, which shows that the polarity of solvents has a remarkable influence on the conversion of **1a** with CO<sub>2</sub>/H<sub>2</sub> in the presence of Au/Al<sub>2</sub>O<sub>3</sub> catalyst.

Subsequently, the effects of some typical supports on catalytic activity were studied for methylation of **1a** with CO<sub>2</sub>/H<sub>2</sub>. The mean size of Au NPs loaded on various supports at around 3 nm was successfully obtained by using the DPU method and sonication-aided impregnation techniques. The typical TEM micrographs and corresponding Au particle size

**Table 1** Effects of different solvent and support on the synthesis of N, N-Dimethylaniline with CO<sub>2</sub>/H<sub>2</sub><sup>a</sup>



Entry	Solvent	Catalyst	Au Size <sup>b</sup> (nm)	Au content <sup>c</sup> (wt %)	Conv. <sup>d</sup> (%)	Sel. <sup>e</sup> (%)
1	Cyclohexane	Au/Al <sub>2</sub> O <sub>3</sub>	2.0	0.73	76	> 99
2	Hexane	Au/Al <sub>2</sub> O <sub>3</sub>	2.0	0.73	61	> 99
3	Toluene	Au/Al <sub>2</sub> O <sub>3</sub>	2.0	0.73	52	> 99
4	1,4-Dioxane	Au/Al <sub>2</sub> O <sub>3</sub>	2.0	0.73	25	96
5	CH <sub>2</sub> Cl <sub>2</sub>	Au/Al <sub>2</sub> O <sub>3</sub>	2.0	0.73	34	> 99
6	THF	Au/Al <sub>2</sub> O <sub>3</sub>	2.0	0.73	29	91
7	Ethanol	Au/Al <sub>2</sub> O <sub>3</sub>	2.0	0.73	12	18
8	Cyclohexane	Au/SiO <sub>2</sub>	3.7	0.97	1	> 99
9	Cyclohexane	Au/α-Mn <sub>2</sub> O <sub>3</sub>	2.4	0.95	1	> 99
10	Cyclohexane	Au/CeO <sub>2</sub>	3.7	0.74	3	> 99
11	Cyclohexane	Au/Co <sub>3</sub> O <sub>4</sub>	4.4	0.96	7	42
12	Cyclohexane	Au/TiO <sub>2</sub>	2.8	1.00	15	> 99
13	Cyclohexane	Au/MgO	2.6	0.91	n.r.	-
14	Cyclohexane	Au/ZnO	2.8	1.00	n.r.	-
15	Cyclohexane	Au/C	4.0	1.00	n.r.	-
16	Cyclohexane	Au powder	150	100	n.r.	-

<sup>a</sup> Reaction conditions: 0.5 mol% Au, N-Methylaniline (1 mmol), CO<sub>2</sub> (1 MPa), H<sub>2</sub> (3 MPa), solvent (10 mL), T = 140 °C, t = 5 h, n. r. = no reaction. <sup>b</sup> Obtained from TEM. <sup>c</sup> Measured by ICP-AES. <sup>d</sup> Conversion and selectivity were determined by GC with n-octane as the internal standard. <sup>e</sup> N-methylformanilide is the only other product.

distributions for these catalysts are shown in Fig. S2. Of the different supports tested, Al<sub>2</sub>O<sub>3</sub> (Table 1, entry 1) provided the best result in terms of high conversion (76%) and excellence selectivity (> 99%). The use of SiO<sub>2</sub>, α-Mn<sub>2</sub>O<sub>3</sub>, CeO<sub>2</sub> and Co<sub>3</sub>O<sub>4</sub> resulted in low yields of **1b** (< 4%) under similar reaction conditions (Table 1, entries 8-11). Moderate yield of **1b** (15%) could be obtained when Au/TiO<sub>2</sub> catalyst was used (Table 1, entry 12). However, **1b** was not detected when MgO, ZnO and C were used as supports (Table 1, entries 13-15). In addition, the use of the Au<sup>0</sup> powder, did not promote the reaction at all (Table 1, entry 16). It was reported that MgO has strong basic character and SiO<sub>2</sub> is an acidic to neutral oxide.<sup>30</sup> Al<sub>2</sub>O<sub>3</sub> with moderate electronegativity can be considered to have both acidic and basic surface sites.<sup>31</sup> These results may suggest that the acid-base properties of the support can affect the catalytic behavior of the supported Au catalysts for methylation of **1a** with CO<sub>2</sub>/H<sub>2</sub>.

Next, the acid-base properties of the typical supported Au catalysts were examined by temperature-programmed desorption (TPD) of NH<sub>3</sub> and CO<sub>2</sub>. As shown in Fig. 1, desorption peaks of NH<sub>3</sub> are observed from Au/Al<sub>2</sub>O<sub>3</sub>, Au/Mn<sub>2</sub>O<sub>3</sub>, Au/TiO<sub>2</sub>, Au/ZnO, Au/CeO<sub>2</sub> and Au/SiO<sub>2</sub>, which indicates that acidic sites exist on these catalysts. From the temperature and intensity of the NH<sub>3</sub> desorption peak, we can

see that Au/Al<sub>2</sub>O<sub>3</sub> possesses relatively strong acidity. No significant acidity, on the other hand, exists on Au/MgO, Au/C and Au/Co<sub>3</sub>O<sub>4</sub>, as no desorption peak of NH<sub>3</sub> can be detected from these catalysts. CO<sub>2</sub>-TPD profiles in Fig. 2 suggest that Au/Al<sub>2</sub>O<sub>3</sub> and Au/MgO both have relatively strong basic sites, whereas no basic sites can be observed on Au/TiO<sub>2</sub>, Au/Co<sub>3</sub>O<sub>4</sub>, Au/C, Au/ZnO and Au/SiO<sub>2</sub>. Weak desorption peaks of CO<sub>2</sub> are detected in Au/Mn<sub>2</sub>O<sub>3</sub> and Au/CeO<sub>2</sub>, which suggests weak basic sites exist on these catalysts. According to the NH<sub>3</sub>-TPD and CO<sub>2</sub>-TPD results, Au/Al<sub>2</sub>O<sub>3</sub> possesses both relatively strong basicity and acidity, while Au/Co<sub>3</sub>O<sub>4</sub> and Au/C have neither acidic nor basic sites. Therefore, we have observed significant support effects in the Au-catalyzed methylation of N-Methylaniline with CO<sub>2</sub>/H<sub>2</sub>, and our studies suggest that the acid-base properties of the supports play important roles in determining both its activity and the selectivity. The strong basicity of supports may promote the adsorption of CO<sub>2</sub> and accelerate departure of product from the surface of catalysts. The strong acidity of supports may be important to anchor the amines (reactive molecules). So the strong acidity and basicity will benefit the methylation reaction.

In summary, acidity and basicity of supports in some typical supported gold catalysts were successfully detected in our experiment and had significant effects on conversion of **1a** and selectivity towards **1b** during direct methylation of **1a** with CO<sub>2</sub>/H<sub>2</sub>. The Au/Al<sub>2</sub>O<sub>3</sub> catalyst with relatively strong acidity and basicity contributes to high conversion of **1a** and excellent selectivity towards **1b**, whereas other catalysts with only strong basic (Au/MgO) or acidic to neutral sites (Au/SiO<sub>2</sub> and Au/C) are almost inactive. Catalysts with weak acid-base properties (Au/Mn<sub>2</sub>O<sub>3</sub> and Au/ZnO) also have no significant activity. There are moderate activity and excellent selectivity when TiO<sub>2</sub> and CeO<sub>2</sub> with a few acidic sites are used as a support in Au/TiO<sub>2</sub> and Au/CeO<sub>2</sub> catalysts. Au/Co<sub>3</sub>O<sub>4</sub> with neutral sites has very low activity and poor selectivity (< 45%) towards **1b**.

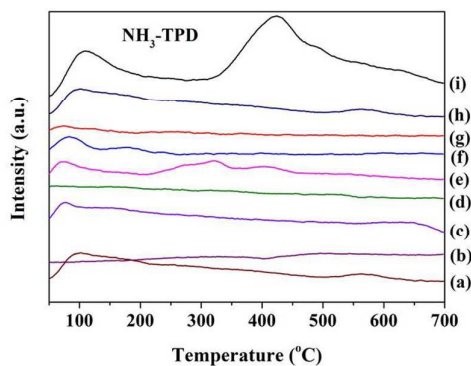


Fig. 1 NH<sub>3</sub>-TPD profiles for some typical supported Au catalysts: (a) Au/CeO<sub>2</sub>, (b) Au/C, (c) Au/ZnO, (d) Au/Co<sub>3</sub>O<sub>4</sub>, (e) Au/Mn<sub>2</sub>O<sub>3</sub>, (f) Au/SiO<sub>2</sub>, (g) Au/MgO, (h) Au/TiO<sub>2</sub>, (i) Au/Al<sub>2</sub>O<sub>3</sub>.

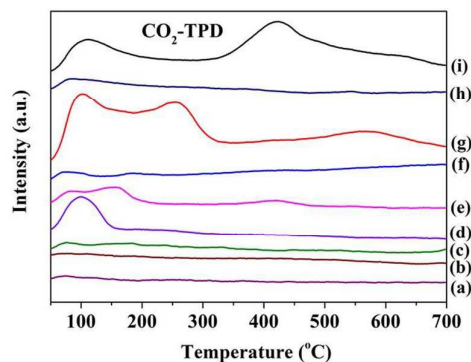


Fig. 2 CO<sub>2</sub>-TPD profiles for some typical supported Au catalysts: (a) Au/C, (b) Au/ZnO, (c) Au/Co<sub>3</sub>O<sub>4</sub>, (d) Au/CeO<sub>2</sub>, (e) Au/Mn<sub>2</sub>O<sub>3</sub>, (f) Au/SiO<sub>2</sub>, (g) Au/MgO, (h) Au/TiO<sub>2</sub>, (i) Au/Al<sub>2</sub>O<sub>3</sub>.

A further study to investigate the effect of reaction parameters was carried out in our experiment. As shown in Fig. 3, the methylation of **1a** with CO<sub>2</sub> and H<sub>2</sub> can be carried out smoothly under relatively mild conditions although the reaction time becomes longer (18 h). It is noteworthy that the selectivity is constant (> 99 %) during the process, which suggests the reaction has high selectivity towards **1b**. Besides, increasing the reaction temperature and pressure respectively can boost the conversion of **1a** to a certain extent (see Fig. S3 and Fig. S4 in the Supporting Information). However, the conversion of **1a** and selectivity towards **1b** kept nearly the same when the total initial pressure and temperature were higher than 4 MPa and 140 °C respectively. Obviously, **1a** could not be fully converted by increasing the total initial pressure or boosting reaction temperature under the present reaction conditions. Nevertheless, **1a** could be fully converted with excellent selectivity towards **1b** when reaction time was up to 18 h under the standard conditions. Therefore, total initial

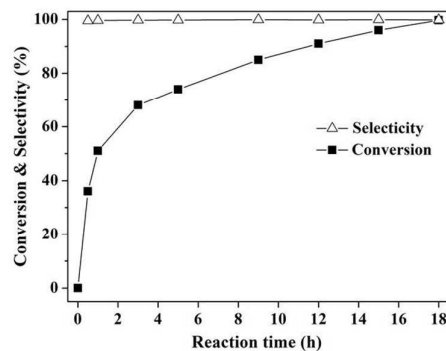
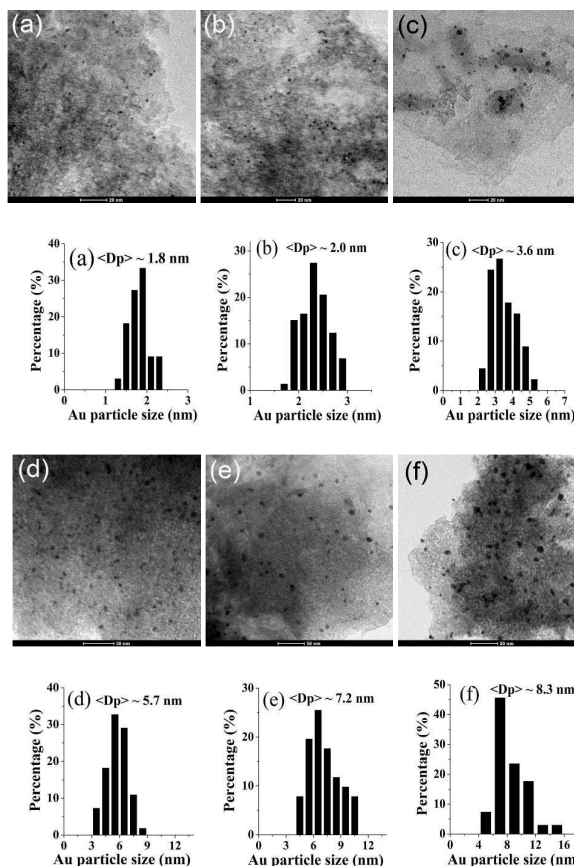


Fig. 3 Effects of reaction time on catalytic activity of Au/Al<sub>2</sub>O<sub>3</sub> catalyst for direct methylation of N-methylaniline with CO<sub>2</sub>/H<sub>2</sub>. Reaction condition: 0.5 mol% Au, 1.0 mmol N-methylaniline, cyclohexane 10 mL, CO<sub>2</sub> (1 MPa), H<sub>2</sub> (3 MPa), T = 140 °C, t = 5 h.

pressure and temperature both affected the yield of **1b** when the reaction time was fixed at 5 h with the yield of **1b** lower than 76%. In order to get **1a** totally converted, prolonged reaction time is required under proper total initial pressure and at appropriate temperature.

#### Preparation and characterization of Au/ $\gamma$ -Al<sub>2</sub>O<sub>3</sub> with controlled mean Au particle sizes

There are still challenges to prepare supported Au catalysts with controlled Au sizes. It was found that aging temperature, aging time and the mole ratio of urea to Au used in DPU process played key roles to obtain controlled Au particle sizes. Louis et al. reported that the pH increased with time due to urea decomposition and most gold was deposited within the first hour in the preparation of Au/TiO<sub>2</sub> by DPU method.<sup>32</sup> Urea begins to decompose when aging temperature is over 60 °C. Compared with Au/TiO<sub>2</sub> prepared by DPU, we found that by regulating aging temperature from 20 to 80 °C in the DPU process could markedly decrease the mean size of Au NPs from 8.3 to 2.0 nm of Au/Al<sub>2</sub>O<sub>3</sub> catalysts (Table 2, entries 1-2, 5). These results clarified that aging temperature used during the DPU process could be an important factor in determining the mean size of Au NPs supported on alumina. As is well known, the rates of nucleation and growth determine the size of a particle formed in the solution. Increasing the aging temperature from 20 to 80 °C can increase the nucleation rates and the pH values in solution because of urea decomposition. At 80 °C, when the mole ratio of urea to Au decreased to 50, the pH value could not reach at 8 as too little urea was added in solution. So a large Au particle size (5.7 nm) was formed (Table 2, entry 3). When aging time was 1 h instead of 6 h, large mean Au NPs size (3.6 nm) was obtained (Table 2, entry 4), indicating that less aging time caused the formation of large Au particle. Alternatively, prolonged aging time favored the formation of small Au particles in the DPU process.<sup>32</sup> However, pH value was over 8 when urea added in solution was enough, which produced the smallest mean Au NPs size (1.8 nm) (Table 2, entry 6). Fig. 4 shows the TEM micrographs and the Au particle size distributions for these



**Fig. 4** TEM micrographs and corresponding Au NPs size distributions for the Au/Al<sub>2</sub>O<sub>3</sub> catalysts with various mean sizes of Au NPs: (a) 1.8 nm, (b) 2.0 nm, (c) 3.6 nm, (d) 5.7 nm, (e) 7.2 nm, and (f) 8.3 nm.

**Table 2** Preparations by deposition-precipitation with urea: influence of aging temperature, aging time and the mole ratio of urea to Au on the mean Au NPs size<sup>a</sup>

Entry	Aging temperature (°C)	Aging time (h)	Mole ratio of urea : Au (mol : mol)	Au loading <sup>b</sup> (wt %)	Mean diameter <sup>c</sup> (nm)
1	20	6	200	0.47	8.3
2	50	6	200	0.46	7.2
3	80	6	50	0.71	5.7
4	80	1	200	0.70	3.6
5	80	6	200	0.73	2.0
6	80	6	400	0.40	1.8

<sup>a</sup> If not mentioned, preparation conditions were: [HAuCl<sub>4</sub>] = 0.48 mmol L<sup>-1</sup>, aging time = 6 h, aging temperature = 80 °C, mole ratio of urea to Au = 200, theoretical Au loading = 1 wt%. <sup>b</sup> Measured by ICP-AES. <sup>c</sup> Obtained from TEM.

Au/Al<sub>2</sub>O<sub>3</sub> samples. Grisel et al. reported the Au loading depended strongly on the final pH of the precipitation solution and a sharp decrease in Au loading was observed with pH value over 8.5.<sup>33</sup> Low Au loadings (yields: < 50%) due to incomplete decomposition of urea in solution were obtained when aging temperatures were below 80 °C (Table 2, entries 1-2). Most Au was loaded on alumina (yield: > 70%) when the mole ratio of urea to gold was less than or equal to 200 at 80 °C (Table 2, entries 3-5). Too much urea added in solution on the other hand caused low Au loading (yield: 40%) because of high pH value over 8.5 (Table 2, entry 6). Thus, regulating pH of the solution during DPU process contributed to the formation of small Au particle and could cause the alteration of Au loadings.

#### Catalytic properties of Au/ $\gamma$ -Al<sub>2</sub>O<sub>3</sub> catalysts with various Au NPs sizes for direct methylation of N-methylaniline with CO<sub>2</sub>/H<sub>2</sub>

The dependence of catalytic activity on the mean size of Au NPs in Au/Al<sub>2</sub>O<sub>3</sub> catalysts prepared by DPU with various preparation parameters was shown in Table 3. The highest yield (83%) of **1b** (Table 3, entry 1) was acquired with the

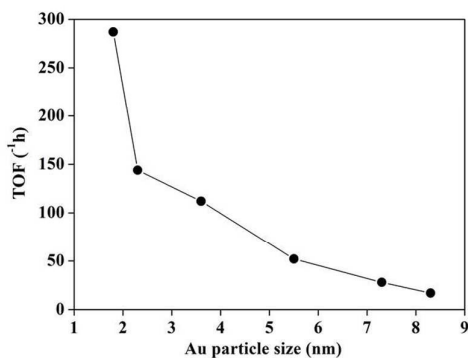


**Fig. 5** Dependence of TOF on the mean Au NPs size for the Au/Al<sub>2</sub>O<sub>3</sub>-catalyzed methylation of N-methylaniline with CO<sub>2</sub>/H<sub>2</sub>. Reaction conditions: catalyst 0.14 g (Au 2.7-5.0 μmol), 1.0 mmol N-methylaniline, cyclohexane 10 mL, CO<sub>2</sub> (1 MPa), H<sub>2</sub> (3 MPa), T = 140 °C.

smallest mean Au NPs size (1.8 nm). Small Au NPs (2.0-5.7 nm) could lead to moderate yields (61-76%) and high selectivity (> 99%) towards **1b** (Table 3, entries 2-7). However, on the other hand, low yields (< 8%) of **1b** (Table 3, entries 8-9) were obtained due to large mean size of Au NPs (> 7.2 nm).

The conversion of **1a** at the initial stages over Au/Al<sub>2</sub>O<sub>3</sub> catalysts was recorded to prove the relations between mean Au NPs size and the intrinsic catalytic reactivity of Au sites. The time course of Au/Al<sub>2</sub>O<sub>3</sub> catalysts was done with different mean Au NPs sizes in the range of 1.8 to 8.3 nm (see Fig. S5 in the Supporting Information). No conversion of **1a** over Al<sub>2</sub>O<sub>3</sub> (Fig. S5) indicates that the Al<sub>2</sub>O<sub>3</sub> species had no active sites for the methylation reaction with CO<sub>2</sub>/H<sub>2</sub>, which shows only the reduced gold species possess active sites for methylation of **1a** with CO<sub>2</sub>/H<sub>2</sub>. The conversion of **1a** increases almost linearly

**Table 3** Catalytic performance of Au/Al<sub>2</sub>O<sub>3</sub> catalysts with various mean Au NPs size from 1.8 to 8.3 nm<sup>a</sup>

Entry	Preparation Conditions <sup>a</sup>	Au loading (wt %)	Au size <sup>c</sup> (nm)	Conv. <sup>d</sup> (%)	Sel. <sup>e</sup> (%)
1	Urea : Au = 400	0.40	1.8	83	> 99
2	Standard condition	0.73	2.0	76	> 99
3	[HAuCl <sub>4</sub> ] = 0.12 mmol L <sup>-1</sup>	0.70	2.4	69	> 99
4	Aging time = 16h	0.65	2.4	70	> 99
5	[HAuCl <sub>4</sub> ] = 1.92 mmol L <sup>-1</sup>	0.60	2.6	63	> 99
6	Aging time = 1 h	0.70	3.6	69	> 99
7	Urea : Au = 50	0.70	5.7	61	> 99
8	Aging temperature = 50 °C	0.46	7.2	8	86
9	Aging temperature = 20 °C	0.47	8.3	6	83

<sup>a</sup> Reaction conditions: catalyst 0.14 g (Au 2.7-5.0 μmol), N-Methylaniline (1 mmol), CO<sub>2</sub> (1 MPa), H<sub>2</sub> (3 MPa), cyclohexane (10 mL), T = 140 °C, t = 5 h. <sup>b</sup> If not mentioned, preparation conditions were: [HAuCl<sub>4</sub>] = 0.48 mmol L<sup>-1</sup>, aging time = 6 h, aging temperature = 80 °C, mole ratio of urea to Au = 200. <sup>c</sup> Obtained from TEM. <sup>d</sup> Conversion and selectivity were determined by GC with n-octane as the internal standard. <sup>e</sup> N-methylformanilide is the only other product.

with reaction time over the initial 30 min in Fig. S5. So we can calculate initial reaction rates by using the slope of the straight line in Fig. S5 for each catalyst. The results are shown in Table S1. Obviously, the initial reaction rates decrease from 5.86 to 0.36 mmol h<sup>-1</sup> g<sup>-1</sup> (cat.) with increasing mean size of Au NPs from 1.8 to 8.3 nm.

Because the gold atoms contribute to the catalytic reactions, we have calculated the TOF (the moles of **1a** converted per unit time at the initial stage per mole total gold atoms) using the initial reaction rate for each Au/Al<sub>2</sub>O<sub>3</sub> catalyst. The results are shown in Fig. 5, suggesting the intrinsic activity per mole total gold atoms decreases with increasing the mean Au NPs size and the methylation of **1a** with CO<sub>2</sub>/H<sub>2</sub> is a structure-sensitive reaction.

The TOF values increase from 114 to 287 h<sup>-1</sup> with decreasing the mean size of Au NPs from 3.6 to 1.8 nm. When the mean sizes of Au NPs are larger than 5.7 nm, the TOF values are lower than 52 h<sup>-1</sup>. The TOF value (about 300 h<sup>-1</sup>) with the best catalyst (with 1.8 nm gold size) is much higher than those measured with other heterogeneous catalysts such as CuAlO<sub>x</sub> (0.1 h<sup>-1</sup>), Pt-MoO<sub>x</sub>/TiO<sub>2</sub> (1.8 h<sup>-1</sup>) and Pd/CuZrO<sub>x</sub> (3.3 h<sup>-1</sup>) for methylation of amines with CO<sub>2</sub>/H<sub>2</sub>.<sup>18-20</sup>

#### Effects of reduction temperature of Au/Al<sub>2</sub>O<sub>3</sub> catalysts on direct methylation of N-methylaniline with CO<sub>2</sub> and H<sub>2</sub>

The as-prepared supported gold precursors are easily reduced to the zero state by thermal treatments with reducing gases or oxidant gases.<sup>34</sup> We previously demonstrated that the very small Au<sup>0</sup> NPs supported on alumina treated with a stream of 5 vol% H<sub>2</sub>/Ar at 350 °C for 2 h showed high catalytic activity for direct methylation of amines with CO<sub>2</sub>/H<sub>2</sub>.<sup>28</sup> In our experiment, the as-prepared Au/Al<sub>2</sub>O<sub>3</sub> precursor of standard Au/Al<sub>2</sub>O<sub>3</sub> catalyst was treated with a stream of 5 vol% H<sub>2</sub>/Ar at 150, 250, 350 and 450 °C respectively for 2 h, at a heating rate of 5 °C min<sup>-1</sup> to obtain Au/Al<sub>2</sub>O<sub>3</sub> samples. The samples were designated as Au/Al<sub>2</sub>O<sub>3</sub>-T, where T denoted the reduction temperature. With these catalysts, the catalytic activity was investigated for direct methylation of amines with CO<sub>2</sub>/H<sub>2</sub>. Table 4 shows that selective production of **1b** in a 38% yield could be achieved when Au/Al<sub>2</sub>O<sub>3</sub>-150 catalyst was used (Table 4, entry 1). An increase in reduction temperature from 150 to

**Table 4** Effects of reduction temperature on catalytic performance of Au/Al<sub>2</sub>O<sub>3</sub> catalyst for direct methylation of N-methylaniline with CO<sub>2</sub>/H<sub>2</sub><sup>a</sup>

Entry	Reduction temperature (°C)	Au size <sup>b</sup> (nm)	Conv. <sup>c</sup> (%)	Sel. <sup>c</sup> (%)
1	150	7.1	38	> 99
2	250	4.5	53	> 99
3	350	2.0	76	> 99
4	450	1.6	67	> 99

<sup>a</sup> Reaction conditions: 0.5 mol% Au, N-Methylaniline (1 mmol), CO<sub>2</sub> (1 MPa), H<sub>2</sub> (3 MPa), cyclohexane 10 mL, T = 140 °C, t = 5 h. <sup>b</sup> Obtained from TEM. <sup>c</sup> Conversion and selectivity were determined by GC with n-octane as the internal standard.

250 °C markedly increased the **1b** yield from 38 to 53% (Table 4, entry 2). The highest yield of **1b** was 76% as reduction temperature of the as-prepared Au/Al<sub>2</sub>O<sub>3</sub> precursor was 350 °C (Table 4, entry 3). However, a further increase of reduction temperature from 350 to 450 °C led to a slight decrease in the desired product yield from 76 to 67% (Table 4, entries 3-4). The high reduction temperature may lead to decrease of the quantities of active hydroxyl group in alumina surface and a weak Au-support interaction in Au/Al<sub>2</sub>O<sub>3</sub>-450 catalyst, which may cause the slight decrease of the catalytic activity.<sup>35</sup> Notably, the selectivity towards **1b** was almost the same, showing that the selectivity did not depend on reduction temperature of the as-prepared Au/Al<sub>2</sub>O<sub>3</sub> precursor.

The factor, which caused different catalytic activities of the Au/Al<sub>2</sub>O<sub>3</sub> catalysts treated by different reduction temperature, could be the change of Au particle size and valence of Au species. To investigate the structure of Au species supported on alumina after the H<sub>2</sub> reduction, Au L<sub>3</sub>-edge XAFS measurement of Au/Al<sub>2</sub>O<sub>3</sub> samples and Au reference compounds was carried out. Fig. 6 shows Au L<sub>3</sub>-edge X-ray absorption near-edge structures (XANES) spectra, which are known to be sensitive to the oxidation states of X-ray absorbing atoms. The XANES features of Au/Al<sub>2</sub>O<sub>3</sub> samples (spectra c-f) after the H<sub>2</sub> reduction with various temperature from 150 to 450 °C are clearly different from that of Au<sub>2</sub>O<sub>3</sub> (spectrum a) but rather similar to that of Au foil (spectrum g), indicating that gold species in these samples are in a reduced state.

Fig. 7 shows the Fourier transform (FT) of extended X-ray absorption fine structure (EXAFS) data of Au/Al<sub>2</sub>O<sub>3</sub> samples reduced at different temperature (150, 250, 350, 450 °C), the Au/Al<sub>2</sub>O<sub>3</sub> precursor, Au foil and Au<sub>2</sub>O<sub>3</sub>. The structural parameters derived from curve-fitting analysis are listed in Table 5. The Au-O coordination number of 3.8 was observed in pure Au<sub>2</sub>O<sub>3</sub>. The EXAFS of the as-prepared Au/Al<sub>2</sub>O<sub>3</sub> precursor (spectrum b) showed the Au-O coordination number (CN) and the Au-Au CN were 1.7 and 3.0 respectively. These results, as reported previously by Grünert et al. for Au/TiO<sub>2</sub>-MCM-48

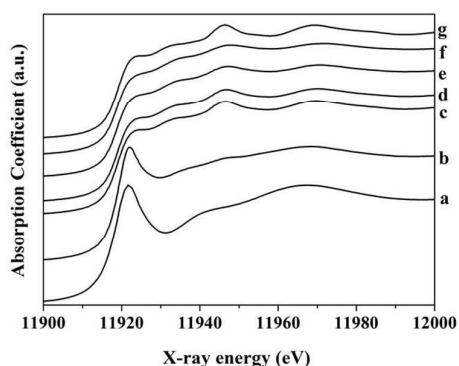


Fig. 6 Au L<sub>3</sub> absorption edge XANES spectra: (a) Au<sub>2</sub>O<sub>3</sub>, (b) as prepared Au/Al<sub>2</sub>O<sub>3</sub> precursor, Au/Al<sub>2</sub>O<sub>3</sub> samples reduced at different temperatures: (c) 150, (d) 250, (e) 350, (f) 450 °C, and (g) Au foil.

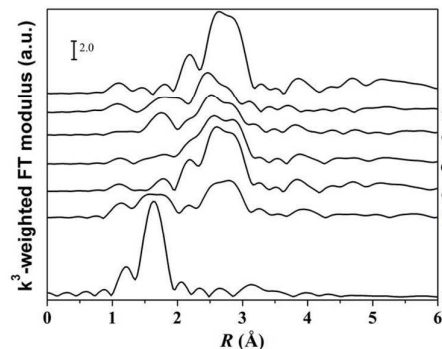


Fig. 7 Au L<sub>3</sub> absorption edge EXAFS Fourier transforms: (a) Au<sub>2</sub>O<sub>3</sub>, (b) the Au/Al<sub>2</sub>O<sub>3</sub> precursor, Au/Al<sub>2</sub>O<sub>3</sub> samples reduced at different temperatures: (c) 150, (d) 250, (e) 350, (f) 450 °C, and (g) Au foil.

catalyst,<sup>36</sup> confirmed that metallic gold species as a minority phase might exist in the as prepared Au/Al<sub>2</sub>O<sub>3</sub> precursor due to auto reduction. After H<sub>2</sub> reduction at various temperature in the range of 150 to 450 °C for 2 h (spectra c-f), the Au-Au CN decreased from 10.7 to 5.6 and the Au-Au bond length decreased from 2.85 to 2.77 Å. It should be noted that there is a significant Au-O path contribution for Au/Al<sub>2</sub>O<sub>3</sub>-T, such as Au/Al<sub>2</sub>O<sub>3</sub>-450. However, this Au-O path has longer length (2.11 ± 0.06 Å) than the Au-O bond in Au<sub>2</sub>O<sub>3</sub>, implying a weak interaction, different from oxidic Au atoms by oxygen, between Au NPs and Al<sub>2</sub>O<sub>3</sub> support. It implies that the oxygen of Au-O bond comes from Al<sub>2</sub>O<sub>3</sub> support. This result can be further suggested from the big uncertainty (± 0.06 Å) of the Au-O path length and the absence of Au oxidation determined by above XANES data. The Au-Au CN in these samples were much less than that in Au foil while close to that in Au/Fe<sub>2</sub>O<sub>3</sub>

Table 5 Fitting parameters of the curve fitted k<sup>3</sup>-weighted EXAFS analysis of the Au/Al<sub>2</sub>O<sub>3</sub>-T samples, the Au/Al<sub>2</sub>O<sub>3</sub> precursor, Au foil and Au<sub>2</sub>O<sub>3</sub>

Samples <sup>a</sup>	Shell	N <sup>b</sup>	R(Å) <sup>c</sup>	σ <sup>2d</sup> (×10 <sup>-3</sup> Å <sup>2</sup> )	ΔE <sub>0</sub> (eV)
Au_foil	Au-Au	11.9 ± 0.5	2.86 ± 0.01	8.1 ± 0.3	3.9
Au/Al <sub>2</sub> O <sub>3</sub> -150	Au-O	0.5 ± 0.2	2.08 ± 0.03	3.0 ± 1.0	-7.0
	Au-Au	10.7 ± 0.9	2.85 ± 0.01	8.8 ± 0.6	3.8
Au/Al <sub>2</sub> O <sub>3</sub> -250	Au-O	0.5 ± 0.2	2.08 ± 0.03	3.0 ± 1.0	-6.9
	Au-Au	10.0 ± 1.2	2.83 ± 0.01	10.1 ± 1.2	3.5
Au/Al <sub>2</sub> O <sub>3</sub> -350	Au-O	0.8 ± 0.3	2.09 ± 0.03	3.0 ± 1.5	-3.4
	Au-Au	7.7 ± 0.8	2.82 ± 0.01	10.0 ± 1.3	4.3
Au/Al <sub>2</sub> O <sub>3</sub> -450	Au-O	0.9 ± 0.3	2.11 ± 0.06	3.5 ± 1.2	-2.0
	Au-Au	5.6 ± 1.4	2.77 ± 0.01	8.9 ± 1.5	0.5
As prepared precursor	Au-O	1.7 ± 0.4	2.02 ± 0.01	5.0 ± 3.0	11.8
	Au-Au	3.0 ± 1.0	2.83 ± 0.01	5.3 ± 2.0	1.8
Au <sub>2</sub> O <sub>3</sub>	Au-O	3.8 ± 0.3	1.99 ± 0.01	2.0 ± 0.7	11.0

<sup>a</sup> Reduction temperature of catalysts. <sup>b</sup> Coordination number. <sup>c</sup> Bond length. <sup>d</sup> Debye-Waller factor.

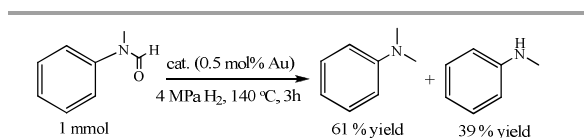
or Au/Fe<sub>2</sub>O<sub>3</sub> catalysts due to the high proportion of surface atoms, suggesting that the small gold NPs supported on alumina were obtained.<sup>37</sup> TEM measurement in Fig. S6 showed that the mean gold NPs size remarkably decreased from 7.1 to 1.6 nm with increasing reduction temperature from 150 to 450 °C. So the TEM result is in good agreement with the XAFS conclusion.

Therefore, the EXAFS and XANES results showed that gold species in the Au/Al<sub>2</sub>O<sub>3</sub> samples were fully reduced after H<sub>2</sub> treatment at different temperature (150, 250, 350, 450 °C) for 2 h. The mean Au NPs size decreased with increasing the reduction temperature from 150 to 450 °C.

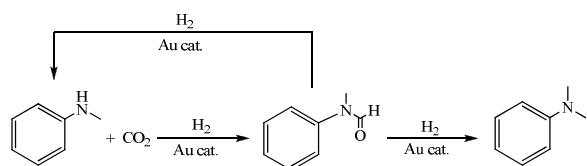
### Reaction mechanism

The group of Shi reported that using Pd/CuZrO<sub>x</sub> under milder conditions or using Pd/ZnZrO<sub>x</sub> during methylation with CO<sub>2</sub>/H<sub>2</sub>, N-formylation mainly processed instead of N-methylation, which indicates the N-formamide could be the intermediate.<sup>20</sup> Beller et al. also reported that formamide was the intermediate during methylation of amines with CO<sub>2</sub>/H<sub>2</sub> catalyzed by Ru catalyst and methanol contributed insignificantly to the reaction.<sup>15b</sup> In order to better understand the mechanism of the methylation reaction catalyzed by the Au/Al<sub>2</sub>O<sub>3</sub> catalyst, control experiments were conducted to confirm the intermediates. Initially, the reduction of the N-methylformanilide (**1c**) with H<sub>2</sub> was investigated in the presence of Au/Al<sub>2</sub>O<sub>3</sub> catalyst. Clearly, **1c** was fully converted and **1b** was the major products in 61% yield (Scheme 1). Aside from methylation of **1c** reduced by H<sub>2</sub>, **1c** was simultaneously reduced by H<sub>2</sub> with Au/Al<sub>2</sub>O<sub>3</sub> catalyst to produce **1a** in 39% yield. Under standard reaction conditions, trace amount of **1c** could be detected. Moreover, we found that increasing the mean size of Au NPs could not only decrease the conversion of **1a**, but also decrease the selectivity towards **1b** to a certain extent as shown in Fig. S7. These results suggest that **1c** could be the key intermediate and significantly contributed to methylation of **1a** with CO<sub>2</sub>/H<sub>2</sub> catalyzed by Au/Al<sub>2</sub>O<sub>3</sub> catalyst.

Based on these results, a plausible mechanism is given in Scheme 2. Under our reaction conditions, the formamide **1c** first produced due to Au-catalyzed reaction of **1a** with CO<sub>2</sub>/H<sub>2</sub>. The formamide **1c** could be quickly reduced to give **1b** (major)



Scheme 1 Control experiment.



Scheme 2 Proposed reaction pathway of Au-catalyzed methylation of **1a** with CO<sub>2</sub>/H<sub>2</sub>.

or be decarbonylated into **1a** (minor). Then, **1a** continued to react with CO<sub>2</sub>/H<sub>2</sub> catalyzed by Au/Al<sub>2</sub>O<sub>3</sub> catalyst following a similar hydrogenation and decarbonylation process as described above to produce the corresponding products.

### Conclusions

Au NPs with uniform mean sizes (~ 3nm) loaded onto various supports were successfully prepared. These supported Au catalysts were studied in detail to clarify the support and Au particle size effects in the direct methylation reaction of N-methylaniline with CO<sub>2</sub>/H<sub>2</sub>. Of the supports tested, Al<sub>2</sub>O<sub>3</sub> with relatively strong acidic and basic surface sites showed the best catalytic performance. Other supports, such as SiO<sub>2</sub> with few acidic sites, Mn<sub>2</sub>O<sub>3</sub> and ZnO with weak acid-base properties, Co<sub>3</sub>O<sub>4</sub> and C with neither acidic site nor basic site and MgO with relatively strong basic sites, have little or low catalytic activity. There is moderate catalytic activity when Au/TiO<sub>2</sub> and Au/CeO<sub>2</sub> with a few acidic sites are used. Supports with relatively strong acid-base bifunctional sites may be necessary for high efficient methylation of N-methylaniline with CO<sub>2</sub>/H<sub>2</sub>.

By changing preparation parameters during the DPU process, we obtained the Al<sub>2</sub>O<sub>3</sub> supported Au NPs with controlled mean sizes in the range of 1.8 to 8.3 nm. We proved that, during the DPU process, aging time, aging temperature and mole ratio of gold to urea were the main preparation parameters affecting the mean size of Au NPs supported on Al<sub>2</sub>O<sub>3</sub>.

The TOF values for direct methylation of N-methylaniline with CO<sub>2</sub>/H<sub>2</sub> increased with decreasing the mean size of Au NPs from 8.3 to 1.8 nm and XAFS results demonstrated that only reduced gold NPs supported on alumina were responsible for high catalytic activity of Au/Al<sub>2</sub>O<sub>3</sub> catalyst. The results suggested that the Au-catalyzed direct methylation of N-methylaniline with CO<sub>2</sub>/H<sub>2</sub> was a structure-sensitive reaction. Then, we proposed that N-methylformanilide could be a key intermediate during methylation of N-methylaniline with CO<sub>2</sub>/H<sub>2</sub>.

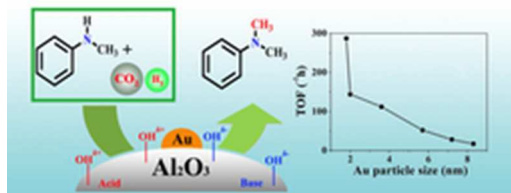
### Acknowledgements

This work was financially supported by the Program of International S&T Cooperation (Grant No. 2014DFG60230), the National Basic Research Program of China (2013CB933104), the National Natural Science Foundation of China (No. 21303246, 11275258, 91127001).

### Notes and references

- J. T. Houghton, G. J. Jenkins and J. J. Ephraums, *Climate Change: The IPCC Scientific Assessment*, Cambridge University Press, Cambridge, UK, 1990.
- H. Arakawa, M. Aresta, J. N. Armor, M. A. Barteau, E. J. Beckman, A. T. Bell, J. E. Bercaw, C. Creutz, E. Dinjus, D. A. Dixon, K. Domen, D. L. DuBois, J. Eckert, E. Fujita, D. H. Gibson, W. A. Goddard, D. W. Goodman, J. Keller, G. J. Kubas, H. H. Kung, J. E. Lyons, L. E. Manzer, T. J. Marks, K. Morokuma, K. M. Nicholas, R. Periana, L. Que, J. R. Nielson,

- W. M. H. Sachtler, L. D. Schmidt, A. Sen, G. A. Somorjai, P. C. Stair, B. R. Stults and W. Tumas, *Chem. Rev.*, 2001, **101**, 953–996.
- 3 T. Sakakura, J. C. Choi and H. Yasuda, *Chem. Rev.*, 2007, **107**, 2365–2387.
- 4 (a) K. M. Y. Yu, I. Curcic, J. Gabriel and S. C. Edman Tsang, *ChemSusChem*, 2008, **1**, 893–899; (b) J. Ma, N. N. Sun, X. L. Zhang, N. Zhao, F. K. Xiao, W. Wei and Y. H. Sun, *Catal. Today*, 2009, **148**, 221–231; (c) W. Wang, S. P. Wang, X. B. Ma and J. L. Gong, *Chem. Soc. Rev.*, 2011, **40**, 3703–3727.
- 5 (a) G. Pagani, *Hydrocarbon Process. Int. Ed.*, 1982, **61**, 87–91; (b) S. Walendy, G. Francio, M. Hoelscher and W. Leitner, *Exp. Green Sustainable Chem.*, 2009, 275–277; (c) S. G. Liang, H. Z. Liu, T. Jiang, J. L. Song, G. Y. Yang and B. X. Han, *Chem. Commun.*, 2011, **47**, 2131–2133; (d) M. Peters, B. Köhler, W. Kuckshinrichs, W. Leitner, P. Markewitz and T. Müller, *ChemSusChem*, 2011, **4**, 1216–1240.
- 6 (a) S. N. Riduan, Y. Zhang and J. Y. Ying, *Angew. Chem. Int. Ed.*, 2009, **48**, 3322–3325; (b) A. E. Ashley, A. L. Thompson and D. O'Hare, *Angew. Chem. Int. Ed.*, 2009, **48**, 9839–9843; (c) S. Wesselbaum, T. vom Stein, J. Klankermayer and W. Leitner, *Angew. Chem. Int. Ed.*, 2012, **51**, 7499–7502.
- 7 K. Motokura, D. Kashiwame, A. Miyaji and T. Baba, *Org. Lett.*, 2012, **14**, 2642–2645.
- 8 Q. Su, J. Sun, J. Q. Wang, Z. F. Yang, W. Q. Cheng and S. J. Zhang, *Catal. Sci. Technol.*, 2014, **4**, 1556–1562.
- 9 Y. Yoshida, Y. Arai, S. Kado, K. Kunimori and K. Tomishige, *Catal. Today*, 2006, **115**, 95–101.
- 10 L. Schmid, A. Canonica and A. Baiker, *Appl. Catal. A*, 2003, **255**, 23–33.
- 11 T. G. Ostapowicz, M. Schmitz, M. Krystof, J. Klankermayer and W. Leitner, *Angew. Chem. Int. Ed.*, 2013, **52**, 12119–12123.
- 12 (a) A. Ricci, *Modern Amination Methods*, Wiley-VCH, Weinheim, 2000; (b) R. N. Salvatore, C. H. Yoon and K. W. Jung, *Tetrahedron*, 2001, **57**, 7785; (c) Z. Rapport, *The Chemistry of Anilines*, Wiley Interscience, 2007.
- 13 (a) M. F. Ali, B. M. ElAli and J. G. Speight, *Handbook of Industrial Chemistry-Organic Chemicals*, McGraw-Hill, New York, 2005; (b) H.-J. Arpe and S. Hawkins, *Industrial Organic Chemistry*, Wiley-VCH, Weinheim, 1997; (c) A. Dhakshinamoorthy, M. Alvaro and H. Garcia, *Appl. Catal. A*, 2010, **378**, 19–25.
- 14 (a) X. Jiang, C. Wang, Y. W. Wei, D. Xue, Z. T. Liu and J. L. Xiao, *Chem. Eur. J.*, 2014, **20**, 58–63; (b) S. Savourey, G. Lefère, J. C. Berthet and T. Cantat, *Chem. Commun.*, 2014, **50**, 14033–14036; (c) I. Sorribes, K. Junge and M. Beller, *Chem. Eur. J.*, 2014, **20**, 7878–7883.
- 15 (a) O. Jacquet, X. Frogneux, C. D. N. Gomes and T. Cantat, *Chem. Sci.*, 2013, **4**, 2127–2131; (b) Y. Li, X. Fang, K. Junge and M. Beller, *Angew. Chem. Int. Ed.*, 2013, **52**, 9568–9571.
- 16 (a) K. Beydoun, T. vom Stein, J. Klankermayer and W. Leitner, *Angew. Chem. Int. Ed.*, 2013, **52**, 9554–9557; (b) Y. Li, I. Sorribes, T. Yan, K. Junge and M. Beller, *Angew. Chem. Int. Ed.*, 2013, **52**, 12156–12160.
- 17 (a) S. Das, F. D. Bobbink, G. Laurency and P. J. Dyson, *Angew. Chem. Int. Ed.*, 2014, **53**, 12876–12879; (b) E. Blondiaux, J. Pouessel and T. Cantat, *Angew. Chem. Int. Ed.*, 2014, **53**, 12186–12190.
- 18 X. J. Cui, X. Dai, Y. Zhang, Y. Deng and F. Shi, *Chem. Sci.*, 2014, **5**, 649–655.
- 19 K. Kon, S. M. A. H. Siddiki, W. Onodera and K. I. Shimizu, *Chem. Eur. J.*, 2014, **20**, 6264–6267.
- 20 X. Cui, Y. Zhang, Y. Q. Deng and F. Shi, *Chem. Commun.*, 2014, **50**, 13521–13524.
- 21 (a) M. Haruta, *Catal. Today*, 1997, **36**, 153–166; (b) X. Zhang, H. Shi and B. Q. Xu, *Angew. Chem. Int. Ed.*, 2005, **44**, 7132–7135; (c) A. Corma, P. Serna and H. García, *J. Am. Chem. Soc.*, 2007, **129**, 6358–6359; (d) L. He, L. C. Wang, H. Sun, J. Ni, Y. Cao, H. Y. He and K. N. Fan, *Angew. Chem. Int. Ed.*, 2009, **48**, 9538–9541; (e) M. D. Hughes, Y.-J. Xu, P. Jenkins, P. McMorn, P. Landon, D. I. Enache, A. F. Carley, G. A. Attard, G. J. Hutchings, F. King, E. H. Stitt, P. Johnston, K. Griffin and C. J. Kiely, *Nature*, 2005, **437**, 1132.
- 22 (a) U. Hartfelder, C. Kartusch, M. Makosch, M. Rovezzi, J. Sá and J. A. van Bokhoven, *Catal. Sci. Technol.*, 2013, **3**, 454–461; (b) K. R. Souza, A. F. F. de Lima, F. F. de Sousa and L. G. Appel, *Appl. Catal. A*, 2008, **340**, 133–139; (c) R. Zanella, S. Giorgio, C.-H. Shin, C. R. Henry and C. Louis, *J. Catal.*, 2004, **222**, 357–367; (d) H.-S. Oh, J. H. Yang, C. K. Costello, Y. M. Wang, S. R. Bare, H. H. Kung and M. C. Kung, *J. Catal.*, 2002, **210**, 375–386; (e) A. Hugon, N. E. Kolli and C. Louis, *J. Catal.*, 2010, **274**, 239–250.
- 23 E. Bus, R. Prins and J. A. van Bokhoven, *Catal. Commun.*, 2007, **8**, 1397–1402.
- 24 M. Shekhar, J. Wang, W. S. Lee, W. D. Williams, S. M. Kim, E. A. Stach, J. T. Miller, W. N. Delgass and F. H. Ribeiro, *J. Am. Chem. Soc.*, 2012, **134**, 4700–4708.
- 25 D. Xiang, X. F. Liu, J. S. Sun, F. S. Xiao and J. M. Sun, *Catal. Today*, 2009, **148**, 383–388.
- 26 L. D. Hao, Y. F. Zhao, B. Yu, H. Y. Zhang, H. J. Xu and Z. M. Liu, *Green Chem.*, 2014, **16**, 3039–3044.
- 27 M. Manzoli, C. Chiorino, F. Vindigni and F. Boccuzzi, *Catal. Today*, 2012, **181**, 62–67.
- 28 X. L. Du, G. Tang, H. L. Bao, Z. Jiang, X. H. Zhong, D. S. Su and J. Q. Wang, *ChemSusChem*, DOI: 10.1002/cssc.201500486.
- 29 X. Q. Li, J. Xu, F. Wang, J. Gao, L. P. Zhou and G. Y. Yang, *Catal. Lett.*, 2006, **108**, 137–140.
- 30 W. H. Fang, J. S. Chen, Q. H. Zhang, W. P. Deng and Y. Wang, *Chem. Eur. J.*, 2011, **17**, 1247–1256.
- 31 K. Shimizu, K. Sugino, K. Sawabe and A. Satsuma, *Chem. Eur. J.*, 2009, **15**, 2341–2351.
- 32 R. Zanella, S. Giorgio, C. R. Henry and C. Louis, *J. Phys. Chem. B*, 2002, **106**, 7634–7642.
- 33 R. J. H. Grisel, P. J. Kooyman and B. E. Nieuwenhuys, *J. Catal.*, 2000, **191**, 430–437.
- 34 G. C. Bond, C. Louis and D. T. Tompson, *Catalysis by Gold*, Imperial College Press, 2006.
- 35 A. Goguet, R. Burch, Y. Chen, C. Hardacre, P. Hu, R. W. Joyner, F. C. Meunier, B. S. Mun, D. Thompsett and D. Tibiletti, *J. Phys. Chem. C*, 2007, **111**, 16927–16933.
- 36 M. W. E. van den Berg, A. De Toni, M. Bandyopadhyay, H. Gies and W. Grünert, *Appl. Catal. A*, 2011, **391**, 268–280.
- 37 (a) Y. Guo, D. Gu, Z. Jin, P. P. Du, R. Si, J. Tao, W. Q. Xu, Y. Y. Huang, S. Senanayake, Q. S. Song, C. J. Jia and F. Schüth, *Nanoscale*, 2015, **7**, 4920–4928; (b) D. P. Akolekar, G. Foran and S. K. Bhargava, *J. Synchrotron Rad.*, 2004, **11**, 284–290.



21x8mm (300 x 300 DPI)